

Geostrophic Adjustment and Restratification of a Mixed Layer with Horizontal Gradients above a Stratified Layer

AMIT TANDON AND CHRIS GARRETT

School of Earth and Ocean Sciences, University of Victoria, Victoria, British Columbia, Canada

(Manuscript received 7 September 1994, in final form 20 January 1995)

ABSTRACT

The restratification of a mixed layer with horizontal density gradients above a stratified layer is considered. Solutions are obtained on the assumption that the width across this front is much larger than the local radius of deformation $\sqrt{\Delta b \bar{h}}/|f|$ based on the buoyancy change across the front Δb , mean mixed layer depth \bar{h} , and the Coriolis parameter f , where b is defined as $-g(\rho - \rho_0)/\rho_0$, but the fractional change in the mixed layer depth is not required to be small. For an initially quiescent mixed layer, created by homogenizing a fluid of constant stratification to a depth that varies horizontally, the isopycnals in the mixed layer tilt about their intersections with the top surface in the adjusted state, and the base of the mixed layer flattens slightly in the frontal region. Other cases considered include mixed layer fronts with initial momentum out of geostrophic balance, created by vertical mixing of a layer with horizontal gradients previously in thermal wind balance. For a wide front, the isopycnals pivot about the middepth for this case. In all cases, for a wide front, the new vertical buoyancy gradient is M^4/f^2 , where $M^2 = |b_x|$ is the magnitude of the horizontal buoyancy gradient, and the Richardson number of the adjusted state is 1, as in an earlier constant depth case.

1. Introduction

Surface layer restratification in a one-dimensional mixed layer model can occur only by an increase in buoyancy by surface processes (such as insolation or precipitation). In the real ocean, horizontal density gradients found in mixed layers created by impulsive mixing by storms can also lead to restratification. In the absence of external forcing leading to further mixing, this new stratification can inhibit further mixing, but the associated velocity shear perhaps could destabilize the flow leading to more mixing. Tandon and Garrett (1994) derived the scaling for the restratification and the Richardson number distribution in a constant depth surface layer. Here our aim is to eliminate the unrealistic assumption of a constant depth, and to solve for the adjusted state for several realistic initial conditions, in both horizontal buoyancy gradients and mixed layer depth variations.

Our aim is to include and improve the representation of the restratification process in currently used mixed layer models. As Young (1994) points out, models that are vertically averaged but horizontally inhomogeneous typically discard the depth-dependent part of the horizontal pressure gradient by assuming that it is bal-

anced precisely by the Reynolds stress terms. These models do not resolve the vertical velocity shear or permit restratification of the surface layer. Ripa (1993) has shown that such averaged systems conserve momentum and energy, but not potential vorticity. Young (1994) proposes a subinertial approximation model that incorporates velocity shear and the dynamical effects of horizontal gradients in density, but assumes a large jump in density across the base of the mixed layer.

In this paper, we examine the restratification in the mixed layer following a single mixing event. Our treatment here differs from our earlier note (Tandon and Garrett 1994) in that the mixed layer is allowed to vary in depth, and is coupled to the dynamics at the interface, and thus to the stratified layer below.

The problem is considered two-dimensional, in the sense that variables are independent of the variable y along the storm track, and three idealized but plausible initial conditions are presented. The first case, labeled I, assumes that a rotating stratified layer at rest with constant stratification N is homogenized in the vertical by a mixing event, which creates a surface mixed layer that is deeper on one side than the other (Fig. 1). Case II assumes a layer with both horizontal and vertical buoyancy gradients, initially in thermal wind balance with isopycnals having the same slope, which is homogenized to a constant depth in momentum and density (Fig. 2). Case III assumes a frontal system initially in thermal wind balance (e.g., Samelson 1993, though we assume different expressions for the basic state), which is homogenized to a constant depth in momen-

Corresponding author address: Dr. Amit Tandon, School of Earth and Ocean Sciences, University of Victoria, P.O. Box 1700, Victoria, BC V8W 2Y2, Canada.
E-mail: tandon@maelstrom.seaoar.uvic.ca

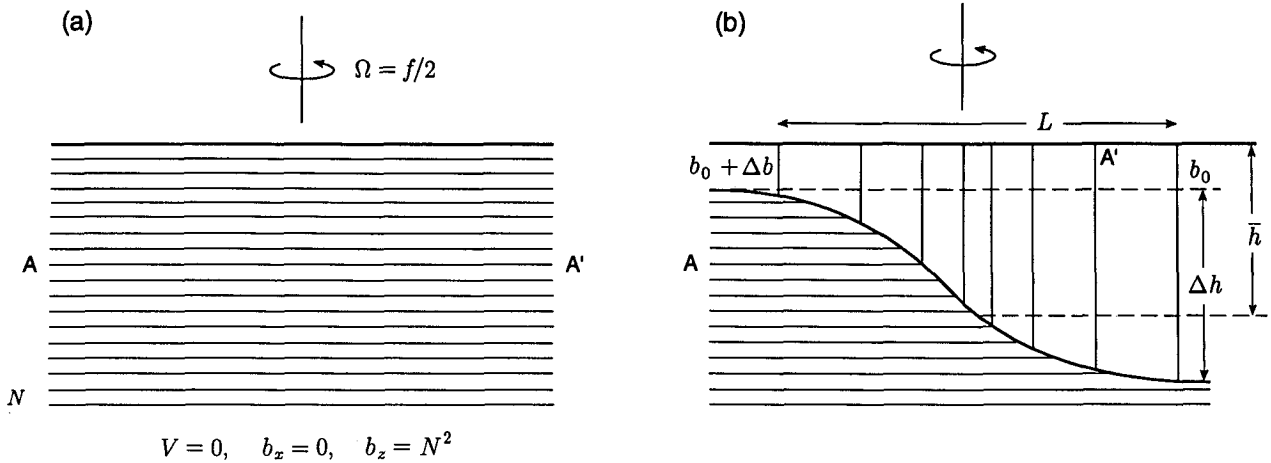


FIG. 1. Case I. An initially stratified layer with buoyancy frequency N before (a) and after (b) an impulsive mixing event.

tum and density (Fig. 3). Cases II and III may be extended to allow for variable mixed layer depth after mixing, but we assume constant depth initially for simplicity. It is also possible to incorporate partial homogenization in the mixed layer, but this brings in extra parameters (Tandon and Garrett 1994), and does not introduce much new understanding of the problem, and so is not considered here.

2. Formulation

a. Case I

Consider a rotating, stratified layer with buoyancy frequency N . The top of the layer is taken to be at $z = 0$. At time $t = 0$, this stratified layer is assumed to be mixed by an impulsive event, with the creation of a well-mixed layer above the remaining stratified layer. The stratified layer is assumed to be initially at rest, and the impulsive mixing is assumed not to impart any momentum but to homogenize the buoyancy field vertically. (We relax this assumption later in cases II and III and consider situations with initial momentum in the mixed layer.) One side of this layer is assumed to mix deeper than the other, and is therefore denser. A frontal region of a variable mixed layer depth connects the two sides. The situation is illustrated in Fig. 1, with the depth of the mixed layer prescribed by $z = -h(x)$. The buoyancy in the mixed layer is therefore

$$b(x) = -\frac{1}{2} N^2 h(x) \tag{1}$$

and in the layer below

$$b(z) = N^2 z. \tag{2}$$

The buoyancy jump at the base of the mixed layer is $N^2 h(x)/2$, and the buoyancy change across the front is $N^2 \Delta h/2$, where Δh is the change in the mixed layer depth across the front. [In the appendix we consider

the situation where the horizontal buoyancy gradients and mixed layer depth do not have this simple relation (1).]

Since the surface layer is not in geostrophic balance, the denser fluid in the mixed layer would tend to tilt isopycnals toward the lighter side, suggesting a tendency to increase the slope of the interface at $z = -h(x)$, though this tendency is opposed by the lower stratified layer. We ask whether the interface steepens or flattens in the geostrophically adjusted steady state and seek to determine the restratification in the mixed layer, and compare it with the results for a mixed layer of constant depth (Tandon and Garrett 1994).

We consider the dynamical balance of the geostrophically adjusted steady state and relate it to the initial position of fluid particles in the mixed layer. This Lagrangian approach was first formulated by Ou (1984) and is extended here to include the dynamics in the stratified layer and at the interface.

We will derive equations for the final position (ξ, ζ) of the particle in terms of its initial position (x, z) . The continuity equation throughout the fluid may be written in terms of the Jacobian of the transformation as

$$\xi_x \zeta_z - \xi_z \zeta_x = 1. \tag{3}$$

We also note that by writing $x = x(\xi, \zeta)$ and differentiating with respect to x and z ,

$$x_\xi \xi_x + x_\zeta \zeta_x = 1, \quad x_\xi \xi_z + x_\zeta \zeta_z = 0. \tag{4}$$

Solving these for x_ξ and x_ζ and using (3) we obtain

$$x_\xi = \zeta_z, \quad x_\zeta = -\xi_z. \tag{5}$$

Similarly, by starting with $z(\xi, \zeta)$, we have

$$z_\xi = -\zeta_x, \quad z_\zeta = \xi_x. \tag{6}$$

Also, throughout the fluid, integration of the x -momentum equation gives

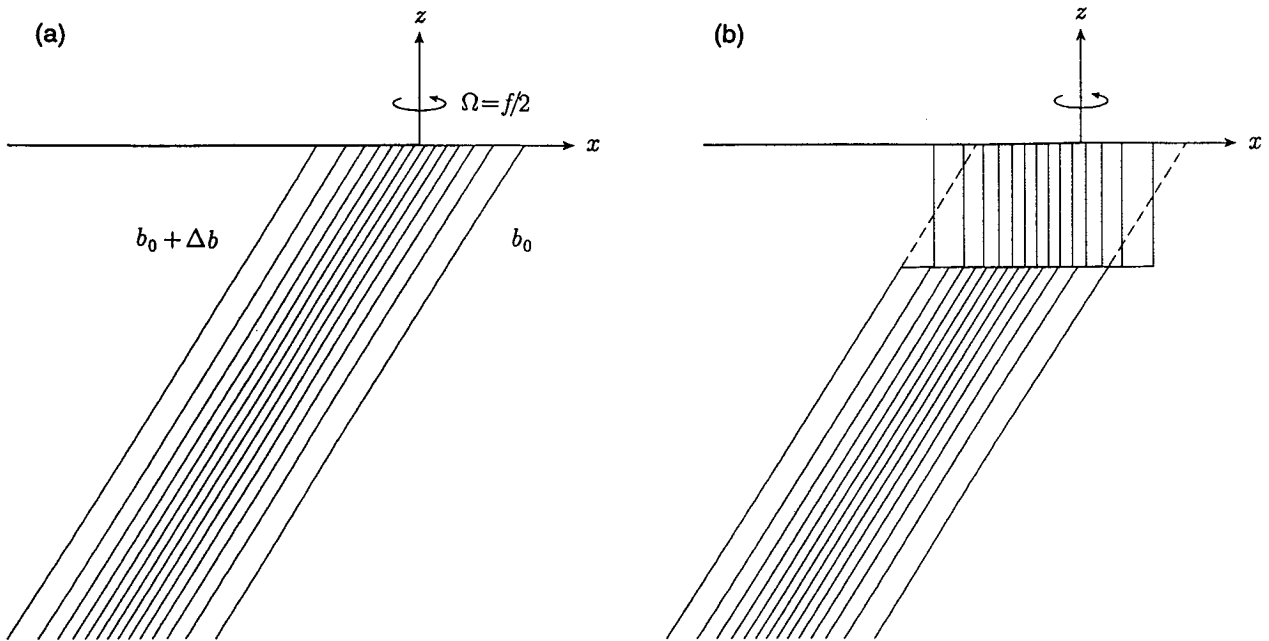


FIG. 2. Case II. (a) The initial state has both horizontal and vertical gradients, but is in thermal wind balance. (b) The isopycnals after an impulsive mixing event.

$$v = -f(\xi - x) \tag{7}$$

and thermal wind balance in the adjusted state requires

$$fv_\zeta = b_\zeta. \tag{8}$$

Substituting (7) for the left-hand side of (8) and expanding the right-hand side,

$$f^2 x_\zeta = b_x x_\zeta + b_z z_\zeta. \tag{9}$$

Using (5) and (6) and noting that $b_z = 0$ in the surface layer and $b_x = 0, b_z = N^2$ in the stratified layer (9) gives

$$\xi_z = -\frac{b_x}{f^2} \zeta_z \tag{10}$$

in the surface layer [as derived by Ou (1984)], and

$$\xi_z = \frac{N^2}{f^2} \zeta_x \tag{11}$$

in the stratified layer.

In the above formulation, the initial state is related to the final state via the time-integrated v -momentum equation (7), rather than by the potential vorticity conservation equation, as is usually done in geostrophic adjustment problems (Gill 1982). It can be easily verified, however, that potential vorticity is conserved since in the final state, $PV = (v_\zeta + f)b_\zeta - v_\zeta b_\xi = fb_z(x_\zeta z_\zeta - x_\zeta z_\xi) = fb_z$, which is the initial PV , where we have used the inverse of the continuity equation (3).

In the final state, the thermal wind balance is satisfied across the interface; that is, Margules' relation holds. At the point (ξ, ζ) on the interface and using superscripts $\hat{\cdot}$ and $\check{\cdot}$ to denote properties just below and just above the interface, respectively, this relation can be written as

$$f[\check{v}(\xi, \zeta) - \hat{v}(\xi, \zeta)] = [\hat{b}(\xi, \zeta) - \check{b}(\xi, \zeta)]S \tag{12}$$

$$= [b(\hat{x}, -h(\hat{x})) - b(\check{x}, -h(\check{x}))]S, \tag{13}$$

since the particles originally at $z = -h(x)$ are assumed to stay on the interface. Here S denotes the slope at the interface. We note that \hat{x} and \check{x} differ, as the displacements above and below the interface to the final position ξ are different (Fig. 4).

Using $v = -f(\xi - x)$ for both layers, (13) becomes

$$f^2(\check{x} - \hat{x}) = N^2 \left[h(\check{x}) - \frac{1}{2} h(\hat{x}) \right] S. \tag{14}$$

The slope S can be calculated in terms of variables above or below. Using variables for the surface layer,

$$\hat{S} = \left. \frac{d\zeta}{d\xi} \right|_{z=-h(\hat{x})}, \tag{15}$$

$$= \frac{\zeta_x - h_x \zeta_z}{\xi_x - h_x \xi_z}. \tag{16}$$

b. Nondimensionalization

The parameters of interest in the problem are $N, f, \bar{h}, \Delta \bar{h}$, and L , the width of the front. Additional param-

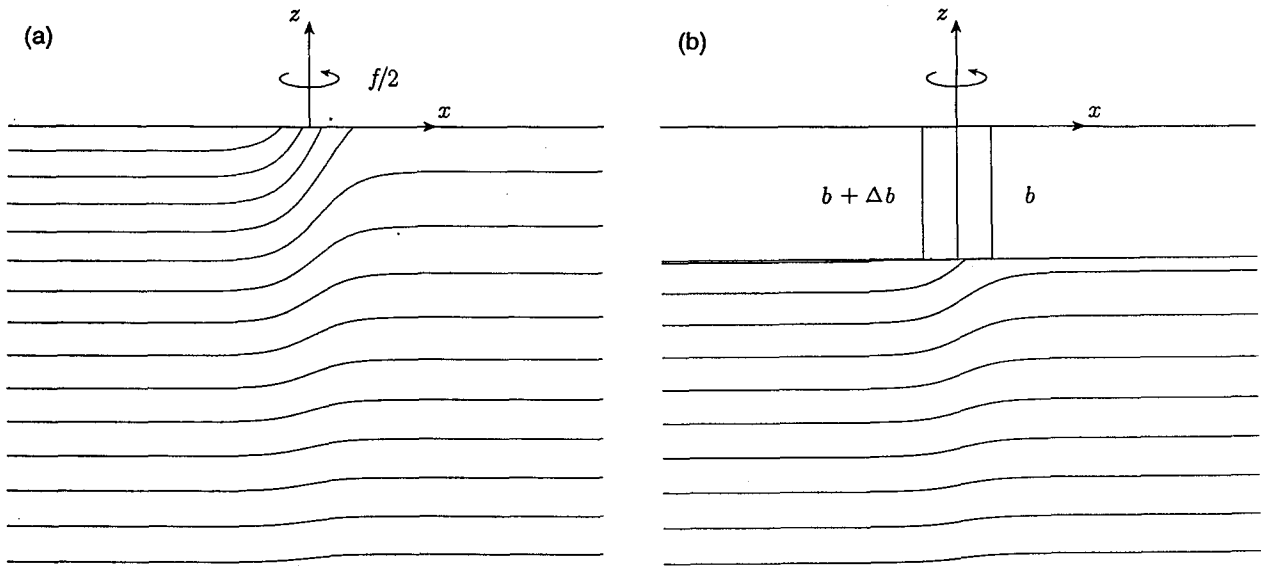


FIG. 3. Case III. (a) The initial state is a frontal system in thermal wind balance and with constant stratification away from the front. (b) The isopycnals after an impulsive mixing event.

eters would result with different initial conditions for the velocity and buoyancy.

For the prototype problem, we choose the buoyancy b to be scaled by $N^2\bar{h}$ and x and ξ to be scaled by $N\bar{h}/f$, while z and ζ are scaled by \bar{h} , and v by $N\bar{h}$. The resulting nondimensional parameters are then

$$\delta = \frac{\Delta\bar{h}}{\bar{h}}, \tag{17}$$

$$\epsilon = \frac{N\bar{h}}{fL}, \tag{18}$$

where δ represents the nondimensional change in the mixed layer depth across the front, and $1/\epsilon$ is the nondimensional width of the front. In the solutions that follow, the parameter δ is $O(1)$, while the front is assumed to be wide so that ϵ is a small parameter.

3. Solution for case I

a. Solution

The continuity equation for the mixed and stratified layers have the same form as their dimensional version

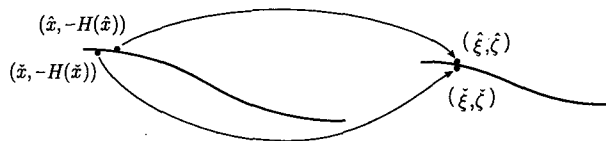


FIG. 4. Schematic showing displacements and nomenclature for the particles above and below the interface.

(3). In nondimensional terms, $b(x) = -\frac{1}{2}h(x)$ in the mixed layer and $b(z) = z$ in the stratified layer. The top boundary is taken to be a rigid lid so that

$$\zeta(x, 0) = 0 \tag{19}$$

and there are no displacements of the particles far away in the geostrophically adjusted state; that is,

$$\xi(x, -\infty) = x, \tag{20}$$

$$\zeta(x, -\infty) = z, \tag{21}$$

$$\xi(\pm\infty, z) = x, \tag{22}$$

$$\zeta(\pm\infty, z) = z. \tag{23}$$

In the surface layer, the nondimensional thermal wind equation (10) becomes

$$\xi_z = -b_x \zeta_z. \tag{24}$$

As shown by Ou (1984), (24) and (3) can be integrated to give

$$\xi(x, z) = A(x) - b_x \zeta(x, z), \tag{25}$$

$$\zeta(x, z) = \frac{A_x - \sqrt{A_x^2 - 2b_{xx}z}}{b_{xx}}, \tag{26}$$

where the minus sign in front of the square root is taken to satisfy (23). Here (25) and (26) constitute the solution in the mixed layer in terms of $A(x)$, which needs to be determined from the matching conditions at the interface and the solution below.

The nondimensional governing equations of the stratified lower layer are

$$\xi_x \zeta_z - \xi_z \zeta_x = 1, \tag{27}$$

and, from (11),

$$\xi_z = \zeta_x. \tag{28}$$

Equations (27) and (28) are not directly integrable for the new position ξ and ζ in the lower layer, so we reformulate the problem in terms of the horizontal displacements

$$\phi(x, z) = \xi - x \tag{29}$$

and vertical displacements

$$\psi(x, z) = \zeta - z \tag{30}$$

in the upper and lower layers. The displacements in the lower layer now satisfy the equations

$$\psi_x = \phi_z, \tag{31}$$

$$\psi_z = -\phi_x + \phi_x \psi_z - \phi_z \psi_x, \tag{32}$$

which are nonlinear in ϕ and ψ . We note that the linear parts represent Cauchy–Riemann conditions for ψ and ϕ . When linearized, the Lagrangian displacements ϕ and ψ , in dimensional form, both satisfy the quasigeostrophic Laplacian equation $f^{-2} \partial_{xx}(\phi, \psi) + N^{-2} \partial_{zz}(\phi, \psi) = 0$.

The Margules relation (13) at the interface takes the form

$$\check{x} - \hat{x} = \left[h(\check{x}) - \frac{1}{2} h(\hat{x}) \right] \hat{S}, \tag{33}$$

where

$$\hat{S} = \frac{\psi_x - h_x(1 + \psi_z)}{1 + \phi_x - h_x \phi_z} \tag{34}$$

evaluated at $\hat{z} = -h(\hat{x})$.

In the surface layer the solution in terms of the displacements is

$$\phi = C(x) - b_x(z + \psi), \tag{35}$$

$$\psi = \frac{1 + C_x - \sqrt{(1 + C_x)^2 - 2b_{xx}z}}{b_{xx}} - z, \tag{36}$$

where the unknown function $A(x)$ has been replaced by the new unknown function $C(x)$ such that $C(x) = A(x) - x$.

We will now solve for the displacements invoking the ‘‘wide-front’’ approximation $\epsilon \ll 1$, which will be justified later in terms of observations. Progress can be made without this approximation using the semigeostrophic approach (Gill 1981), but this makes the problem quite complicated due to Margules’s condition at the interface and is not pursued here. The depth of the mixed layer is given by $h(x) = 1 + \delta H(\epsilon x)$, and anticipating that the displacements will also vary over the longer scale ϵ^{-1} , we use multiple scale expansions in

x , with x and ϵx as the new length scales. Then, for example, $h(x, \epsilon x) = h(\epsilon x) = 1 + \delta H(\epsilon x)$ and $h_x = \epsilon \delta H'$, where the prime represents derivative with respect to ϵx .

Boundary conditions (20) and (22) applied to (35) with the wide-front condition suggest that $C = C(\epsilon x)$ and is $O(1)$ or smaller. From (35) and (36) then, the displacements vary over ϵ^{-1} , so that $\phi = \phi(\epsilon x, z)$ and $\psi = \psi(\epsilon x, z)$, and have no far-field variation.

Since b_x and C_x are both $O(\epsilon)$ (or smaller), (36) shows that ψ is also $O(\epsilon)$. In fact, expanding (35) and (36) in powers of ϵ gives the displacements in the upper layer as

$$\phi(\epsilon x, z) = C + \frac{1}{2} \epsilon \delta H' z + O(\epsilon^2) \tag{37}$$

$$\psi(\epsilon x, z) = -\epsilon C' z + O(\epsilon^2). \tag{38}$$

The restratification in the final state is

$$b_{\check{z}} = b_x x_{\check{z}} \tag{39}$$

$$= -b_x \phi_z, \tag{40}$$

using (5) and (29), and

$$= b_x^2 [1 + O(\epsilon)],$$

using (37). Thus, in dimensional terms $N^2 = (M^4/f^2)[1 + O(\epsilon)]$ showing that the new stratification is the same as in the constant depth problem (Tandon and Garrett 1994). For the displacements, the lowest-order solutions are now known except for the depth-independent part $C(\epsilon x)$, which remains to be determined from the solution below and the matching conditions at the interface.

From equations (37) and (38), and using $h = 1 + \delta H(\epsilon x)$, we can now evaluate the interface slope as

$$\hat{S} = -\epsilon \delta H' + O(\epsilon^2). \tag{42}$$

The Margules relation (33) now becomes

$$\check{x} - \hat{x} = \left[\frac{1}{2} + \delta H(\epsilon \check{x}) - \frac{1}{2} \delta H(\epsilon \hat{x}) \right] \times (-\epsilon \delta H') + O(\epsilon^2). \tag{43}$$

This shows that $\check{x} - \hat{x}$ is $O(\epsilon)$, so that to $O(\epsilon^2)$, $H(\epsilon \check{x})$ may be replaced by $H(\epsilon \hat{x})$ in (43) and

$$\check{x} - \hat{x} = -\frac{1}{2} \epsilon \delta H' (1 + \delta H) + O(\epsilon^2), \tag{44}$$

where H, H' are in terms of $\epsilon \hat{x}$.

Since the fluid particles at \hat{x} and \check{x} are at ξ in the adjusted state (Fig. 4),

$$\hat{x} + \hat{\phi} = \check{x} + \check{\phi}, \tag{45}$$

$$\hat{\psi} + \hat{z} = \check{\psi} + \check{z}, \tag{46}$$

or

$$\hat{\psi} - \delta H(\hat{x}) = \check{\psi} - \delta H(\check{x}). \quad (47)$$

Rewriting (44) in terms of displacements by using (45)

$$\begin{aligned} \check{\phi}(\check{x}, -h(\check{x})) &= \hat{\phi}(\hat{x}, -h(\hat{x})) \\ &+ \frac{1}{2} \epsilon \delta H'(1 + \delta H) + O(\epsilon^2). \end{aligned} \quad (48)$$

Using (37) for $\hat{\phi}$, the $O(\epsilon)$ contributions cancel out! We are now left with

$$\check{\phi} = C(\epsilon \hat{x}) + O(\epsilon^2). \quad (49)$$

Similarly, using (47),

$$\begin{aligned} \check{\psi}(\check{x}, -h(\check{x})) &= \hat{\psi}(\hat{x}, -h(\hat{x})) \\ &+ \delta H(\epsilon \check{x}) - \delta H(\epsilon \hat{x}), \end{aligned} \quad (50)$$

$$= \epsilon C'(1 + \delta H) + O(\epsilon^2). \quad (51)$$

We have now derived the forcing (horizontal and vertical displacements) given by (49) and (51) that the lower layer is subjected to by the upper layer in terms of the unknown function $C(\epsilon \hat{x})$.

The governing equations are coupled for ϕ and ψ in the layer below and need to be solved to find the solution and C . In the stratified layer, ϕ and ψ are coupled by the governing equations, due to the forcing by the top layer, (49) and (51).

It is easy to see that there are no displacements ϕ and ψ for large z in the stratified layer for this problem. Thus the relevant scale at which displacements occur is γz , where $\gamma = \gamma(\epsilon)$ signifies the "depth of influence." Substitution in the governing equations then implies that $\gamma = \epsilon$ under the wide-front assumption. This assumption also linearizes the governing equations, implying that ψ and ϕ are mutually orthogonal and are Laplacian to the lowest order.

Now, the forcing condition in ψ , (51), implies that $\check{\psi}$ has to be $O(\epsilon)$ or smaller at the interface. Since ψ satisfies Laplace's equation in the lower layer, ψ must be $O(\epsilon)$ or smaller everywhere. Also, ϕ must be the same order as ψ in the region of interest, from (49), and hence, C must be $O(\epsilon)$ or smaller; that is,

$$C(\epsilon \hat{x}) = \epsilon C_1(\epsilon \hat{x}) + \epsilon^2 C_2(\epsilon \hat{x}) + O(\epsilon^3). \quad (52)$$

We can repeat this argument once again since ψ is now forced at $O(\epsilon^2)$ from (51) and (52), and so in the stratified layer ϕ , and hence $C(\epsilon \hat{x})$, must arise at $O(\epsilon^2)$, or

$$C(\epsilon \hat{x}) = \epsilon^2 C_2(\epsilon \hat{x}) + O(\epsilon^3)! \quad (53)$$

We can pursue these expansions at the next order to show that ψ arises at $O(\epsilon^2)$ due to a forcing independent of C at the interface, or ψ can be determined by solving

$$\psi_{xx} + \psi_{zz} = 0 \quad (54)$$

subject to the boundary condition that at the interface $\check{z} = -[1 + \delta H(\epsilon \check{x})]$, from (38) and (47),

$$\begin{aligned} \psi(\epsilon \check{x}) &= -\frac{1}{4} \epsilon^2 \delta (1 + \delta H)^2 H'' \\ &- \frac{1}{2} \epsilon^2 \delta^2 H'^2 (1 + \delta H). \end{aligned} \quad (55)$$

Again, ϕ arising at $O(\epsilon^2)$ can then be determined from Cauchy-Riemann conditions to within a constant which can be determined by far-field conditions. Hence by using (49) $C_2(\epsilon \hat{x})$ can be determined.

The process above can now be used to determine the solutions to higher order, but what is remarkable is that we now know the solutions to the lowest order. From (37) and (53) the solution at the lowest order in the mixed layer is

$$\phi(\epsilon x, z) = \frac{1}{2} \epsilon \delta H' z, \quad (56)$$

and from (36) and (53),

$$\psi(\epsilon x, z) = -\frac{1}{4} \epsilon^2 \delta H'' z^2. \quad (57)$$

The stratified layer below has horizontal and vertical displacements at $O(\epsilon^2)$, and therefore the lower layer remains quiescent at the lowest order. This solution is sketched in Fig. 5. To the lowest order, the isopycnals just tilt in the horizontal, pivoted about the top surface, and there is no vertical displacement at $O(\epsilon)$. The interface flattens in the central region, changing its depth by $O(\epsilon^2)$, and the vertical displacements at this order arise to satisfy continuity. [For instance, it is easy to check that $\int_{-1}^0 \phi(0, z) dz = -\epsilon \delta H'(0)/4 = \int_{-\infty}^0 \psi(x, z) dz = -1$.] Also, the top surface is a constant pressure surface to $O(\epsilon)$, unlike the adjustment problem in Ou (1984), where the middepth surface in the geostrophically adjusted state turns out to be a constant pressure surface. Since C is $O(\epsilon^2)$, the mixed layer restratification for this case in (41) is the same to the next order; that is, $b_\zeta = b_x^2 / f^2 + O(\epsilon^4)$.

b. Energetics

The fraction of the available potential energy in the mixed layer that is radiated away is found using the lowest-order solutions. We essentially follow Ou (1986). The top surface is considered to be rigid lid and so does not contribute to the change in the available potential energy.

In dimensional terms, from (56) and (57) of the previous section,

$$\phi = \frac{1}{2} \lambda^2 \bar{h}^{-2} h_x z \quad (58)$$

$$\psi = -\frac{1}{4} \lambda^2 \bar{h}^{-2} h_{xx} z^2, \quad (59)$$

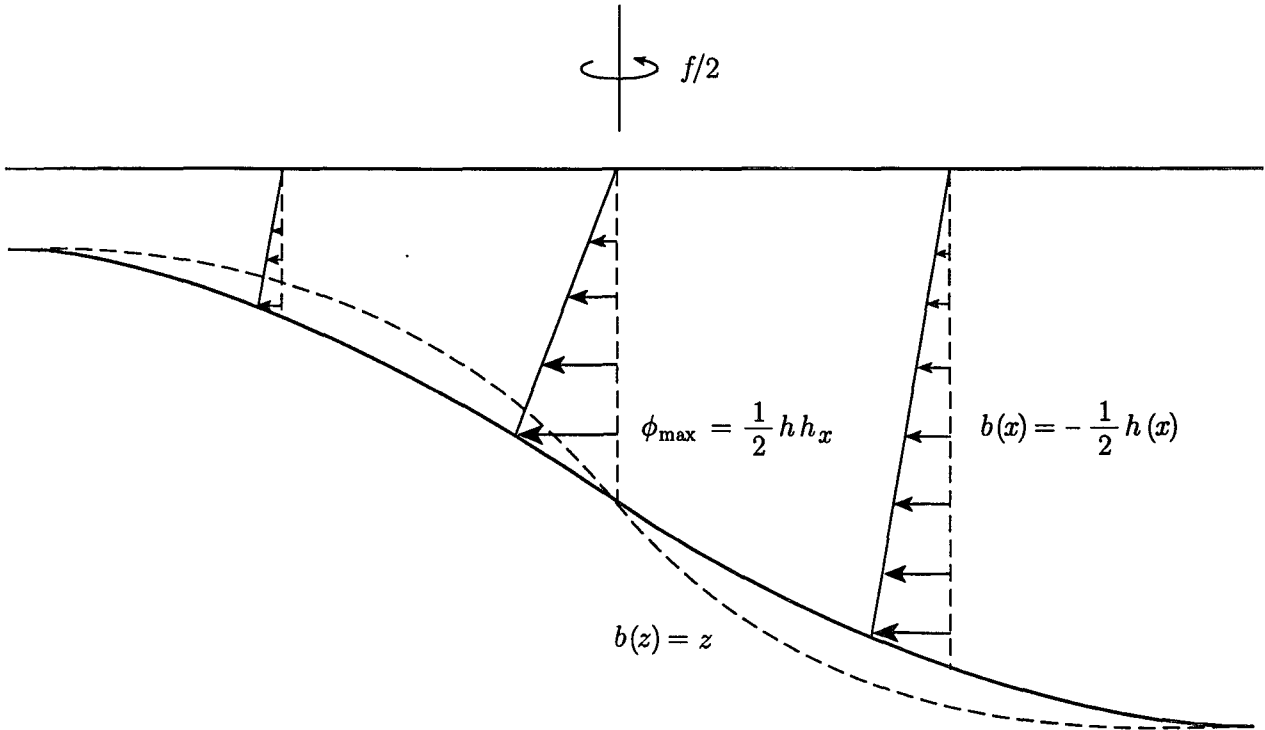


FIG. 5. Solution for case I. The interface flattens in the central region and isopycnals tilt with the top surface as a pivot surface.

where $\lambda = N\bar{h}/f$ is the radius of deformation. From (55), the vertical displacement at the interface in the stratified layer is

$$\check{\psi}(x, -h) = -\frac{1}{4} \lambda^2 \bar{h}^{-2} (h^2 h_{xx} + 2hh_x^2). \quad (60)$$

Further, the total change in the potential energy is

$$\Delta PE = \int_{-\infty}^{\infty} \int_{-\infty}^0 \rho_0 b \psi dx dz \quad (61)$$

and the change in the kinetic energy is

$$\Delta KE = \frac{1}{2} \int_{-\infty}^{\infty} \int_{-\infty}^0 \rho_0 v^2 dz dx, \quad (62)$$

where ρ_0 is a reference density.

The potential energy released in the mixed layer during the adjustment process to $O(\epsilon)$ is given by

$$\Delta PE_1 = \rho_0 \int_{-\infty}^{\infty} \int_{-h(x)}^0 b \psi dx dz \quad (63)$$

$$= \frac{1}{24} \rho_0 N^2 \lambda^2 \bar{h}^{-2} \int_{-\infty}^{\infty} h_{xx} h^4 dx \quad (64)$$

$$= -\frac{1}{6} \rho_0 N^2 \lambda^2 \bar{h}^{-2} \int_{-\infty}^{\infty} h_x^2 h^3 dx. \quad (65)$$

Note that the particles on the denser side in the surface layer move upward, and those on the less dense side

move downward, thus raising the potential energy in the surface layer and giving $\Delta PE_1 < 0$.

The gain in kinetic energy after reaching the adjusted steady state is

$$\Delta KE = \frac{1}{2} \rho_0 f^2 \int_{-\infty}^{\infty} \int_{-h(x)}^0 \phi^2 dz dx \quad (66)$$

$$= \frac{1}{24} \rho_0 N^2 \lambda^2 \bar{h}^{-2} \int_{-\infty}^{\infty} h_x^2 h^3 dx, \quad (67)$$

where we have neglected the kinetic energy in the stratified layer, since it is $O(\epsilon^2)$ whereas (65) and (67) are $O(\epsilon)$ to the lowest order.

In the stratified layer, the potential energy change is given by

$$\Delta PE_2 = \rho_0 N^2 \int_{-\infty}^{\infty} \int_{-\infty}^{-h(x)} z \psi dx dz. \quad (68)$$

The double integral above can be evaluated by integrating twice wrt z ,

$$\begin{aligned} \int_{-\infty}^{\infty} \int_{-\infty}^{-h(x)} z \psi dx dz &= \frac{1}{2} \int_{-\infty}^{\infty} \check{\psi}(x, -h) h^2 dx \\ &+ \frac{1}{6} \int_{-\infty}^{\infty} \check{\psi}_z(x, -h) h^3 dx + \frac{1}{6} \int_{-\infty}^{\infty} \int_{-\infty}^{-h(x)} \psi_{zz} z^3 dz dx. \end{aligned} \quad (69)$$

The first term on the rhs of (69) is $O(\epsilon)$, the second is $O(\epsilon^2)$, and the third term is $O(\epsilon^3)$ as shown below.

Using (54) and reordering the limits of integration, the third term on the rhs of (69) is

$$-\int_{-\infty}^{h_{\max}} \frac{1}{6} z^3 \int_{-\infty}^{+\infty} \psi_{xx} dx dz - \int_{h_{\min}}^{h_{\max}} \frac{1}{6} h^3 \int_{-\infty}^{x(h)} \psi_{xx} dx dh \quad (70)$$

$$= 0 - \int_{h_{\min}}^{h_{\max}} \frac{1}{6} h^3 \psi_x(x(h), h) dh, \quad (71)$$

which is $O(\epsilon^3)$ as ψ is $O(\epsilon^2)$ and $h_{\max} = h(+\infty)$ and $h_{\min} = h(-\infty)$.

To leading order, therefore, the change in potential energy in the stratified layer using (60) is

$$\Delta PE_2 = \frac{1}{2} \rho_0 N^2 \int_{-\infty}^{\infty} \psi(x, -h) h^2 dx \quad (72)$$

$$= -\frac{1}{8} \rho_0 N^2 \lambda^2 \bar{h}^{-2} \left(\int_{-\infty}^{\infty} h_{xx} h^4 dx + 2 \int_{-\infty}^{\infty} h_x^2 h^3 dx \right) \quad (73)$$

$$= \frac{1}{4} \rho_0 N^2 \lambda^2 \bar{h}^{-2} \int_{-\infty}^{\infty} h_x^2 h^3 dx. \quad (74)$$

Thus, to leading order, of the available potential energy released in the stratified layer, two-thirds is used to raise the potential energy of the surface layer, one-sixth remains as kinetic energy, and one-sixth is radiated away as inertial waves. Of the total available potential energy change in both layers, one-half remains as the kinetic energy and one-half radiates away.

Note that the higher-order contributions to the energy occur both due to higher-order terms in ϕ and ψ (above and below) and due to interfacial displacement terms (changing domain).

Our estimates show that this adjustment process is not a significant source of internal waves for small values of the deformation radius λ . The potential energy radiated per unit distance in y as inertial waves away from the region of adjustment is $(1/24)\rho_0 N^2 \lambda^2 \bar{h}^{-2} \times \int_{-\infty}^{\infty} h_x^2 h^3 dx$, of the order $(1/24)\rho_0 \epsilon f^2 \lambda^3 \bar{h} \delta^2$. With $\delta = 1$, $\lambda = 4$ km (and $L = 20$ km so that $\epsilon = 0.2$), $f = 10^{-4} \text{ s}^{-1}$, and $\bar{h} = 100$ m, this potential energy radiation is about $5 \times 10^5 \text{ J m}^{-1}$. If this happens in only three inertial periods, over the frontal width of 20 km, but with average spacing between fronts of 100 km, the downward energy flux is of the order $3 \times 10^{-5} \text{ W m}^{-2}$, which is small compared with various estimates (Olbers 1983) that show the energy flux associated with internal waves is of the order $1 \times 10^{-3} \text{ W m}^{-2}$.

4. Solutions for cases II and III

The mixed layer base for the initial condition is taken to be fixed at $z = -h$, though variations in depth can be treated as in case I. The profiles of velocity $v(x, z)$

before the storm is assumed to be in thermal wind balance with the profile $b(x, z)$ for cases II and III. We denote the variables with subscript 1 for the mixed layer and subscript 2 for the stratified layer below. We do not use these subscripts on the displacements ϕ and ψ , as it is clear in the remaining section which layer is being considered. Impulsive mixing is assumed to homogenize the velocity and buoyancy fields vertically in the mixed layer to depth h , and the homogenized values after the event are called $v_1(x)$ and $b_1(x)$, respectively.

The buoyancy is nondimensionalized by the horizontal buoyancy difference Δb across the layer. The x and ξ coordinates are scaled by $\lambda = \sqrt{\Delta b h}/f$, z and ζ by h , and velocities by $f\lambda$. The frontal-width parameter is now

$$\epsilon = \frac{\sqrt{\Delta b h}}{fL} = \frac{\lambda}{L}, \quad (75)$$

where L is the width of the front, and we assume that this is a small parameter. The width parameter ϵ , defined for cases II and III in (75), differs from our definition (18) for case I by a factor $\sqrt{\delta}/2$, but δ is $O(1)$, so the two definitions are equivalent.

For illustration, case II can be assumed to have a profile for the nondimensional buoyancy of the form

$$b(x, z) = -\frac{1}{2} \left[\tanh \epsilon \left(x - \frac{z}{s} \right) \right] \quad (76)$$

and for case III, assuming that $N^2 h = \Delta b$,

$$b(x, z) = z - \frac{1}{2} [\tanh(\epsilon x)] e^{\beta z}. \quad (77)$$

These profiles are schematically shown in Figs. 2 and 3. For case II, $\partial b_2/\partial x$ and $\partial b_2/\partial z$ in the initially undisturbed lower layer are related by the scaled slope s of the isopycnals, which is taken to be $O(1)$. Therefore, $\partial b_2/\partial z$ is $O(\epsilon)$ in the lower layer for case II. For case III, $\partial b_2/\partial z$ is $O(1)$ in the lower layer.¹ The profiles in the mixed layer after mixing can be found by depth averaging (76) and (77) from $z = -1$ to $z = 0$. In the lower layer, $\text{Ri} = 1/\epsilon$ for case II, while it is $1/\epsilon^2$ in case III.

The form of the continuity equation (3) remains the same. Using nondimensional versions of (5) and (8) and the integrated x -momentum equation,

$$v = v_1(x) - f(\xi - x), \quad (78)$$

the dimensionless thermal wind equation is

$$-\xi_z(1 + v_{1x}) = b_{1x} \zeta_z. \quad (79)$$

This can be integrated over z as before, and as in Ou (1984), to give

¹ We assume here that $2 - \beta$ is larger than $O(\epsilon)$.

$$\xi(x, z) = \frac{A(x) - b_{1x}\zeta}{1 + v_{1x}}, \quad (80)$$

and after substituting this into (3) and integrating,

$$\zeta(x, z) = \frac{-E \pm \sqrt{E^2 + 2F(1 + v_{1x})^2 z}}{F}, \quad (81)$$

where

$$E = A_x(1 + v_{1x}) - Av_{1xx}, \quad (82)$$

$$F = b_{1x}v_{1xx} - (1 + v_{1x})b_{1xx}. \quad (83)$$

We can again write $A(x) = x + C(\epsilon x)$ with C no larger than $O(1)$ as before, and with primes denoting differentiation with ϵx , we get

$$E = 1 + \epsilon(C' + v'_1) + O(\epsilon^2) \quad (84)$$

$$F = -\epsilon^2 b''_1, \quad (85)$$

and hence $F(1 + v_{1x})^2 z/E^2$ is $O(\epsilon^2)$. We can now expand (80) and (81) to get

$$\phi(x, z) = C(x)(1 - \epsilon v'_1) - \epsilon v'_1 x - \epsilon b'_1 z + O(\epsilon^2) \quad (86)$$

$$\psi(x, z) = \epsilon(v'_1 - C')z. \quad (87)$$

It is clear that, in the final state in dimensional form,

$$b_\zeta = b_{1x}x_\zeta = -b_{1x}\phi_z = \frac{b_{1x}^2}{f^2} + O(\epsilon^3). \quad (88)$$

Hence, dimensionally the restratification is M^4/f^2 to the lowest order as before; the unknown function C is only a function of ϵx .

We now consider the dynamics in the lower layer to complete the solution for the displacements to the lowest order. The alongfront momentum equation can be integrated as before to give at the interface

$$\hat{v}(\xi, \zeta) = v_1(\hat{x}, -1) - \phi(\hat{x}, -1), \quad (89)$$

$$\check{v}(\xi, \zeta) = v_2(\check{x}, -1) - \phi(\check{x}, -1), \quad (90)$$

so that the Margules relation at the interface can be written to give

$$v_2(\check{x}, -1) - v_1(\hat{x}, -1) + \hat{\phi}(\hat{x}, -1) - \check{\phi}(\check{x}, -1) = [b_1(\hat{x}) - b_2(\check{x})]S, \quad (91)$$

where S is the slope at the interface at position (ξ, ζ) . From (16), to the lowest order in ϵ , S is $\epsilon^2(C'' - v''_1)$ if the mixed layer depth is taken to be initially uniform. Thus to $O(\epsilon)$, the coupling at the interface is

$$\hat{\phi} - \check{\phi} = v_1(\hat{x}, -1, 0) - v_2(\check{x}, -1, 0). \quad (92)$$

In both cases II and III $\hat{x} - \check{x} = \hat{\phi} - \check{\phi}$ is $O(\epsilon)$ from the rhs of (92). Thus (92) becomes

$$\hat{\phi} - \check{\phi} = v_1(\hat{x}, -1, t = 0) - v_2(\check{x}, -1, t = 0) + O(\epsilon^2), \quad (93)$$

$$= v_{\text{jump}}(\hat{x}) + O(\epsilon^2), \quad (94)$$

where $v_{\text{jump}}(\hat{x})$ is the initial velocity difference between the bottom of the mixed layer and top of the stratified layer. This is $O(\epsilon)$ for both cases II and III. If the slope of the mixed layer changes slowly as in case I, the coupling condition above can be modified by the addition of the term $-[b_1(\hat{x}) - b_2(\check{x})]\partial h/\partial x$ to the rhs of (91).

Now, as in case I, we consider the dynamics in the lower layer. The continuity equation for the stratified layer, written in terms of the isopycnal displacement fields ϕ and ψ is, as before,

$$\phi_x + \psi_z - \phi_z\psi_x + \phi_x\psi_z = 0. \quad (95)$$

In the lower layer, we can use nondimensional versions of (8), $fv_{2z} = b_{2x}$, and $v = v_2 - f(\xi - x)$ with (5) and (6) to yield the thermal wind balance in terms of the displacements as

$$\frac{\partial b_2}{\partial x}(\phi_x - \psi_z) + \frac{\partial b_2}{\partial z}\psi_x - \phi_z\left(1 + \frac{\partial v_2}{\partial x}\right) = 0. \quad (96)$$

In case I, this reduces to $\psi_x = \phi_z$, and in the stratified layer the displacements ϕ and ψ are both $O(\epsilon^2)$ in the horizontal and vertical. However, since the dynamics in the lower layer may not reduce to a Laplacian in cases II and III, the displacements ϕ and ψ below can arise at different orders in ϵ . Thus we formally expand the displacements as

$$\phi = \phi_0(\epsilon x, \delta z) + \epsilon\phi_\epsilon(\epsilon x, \delta z) + \delta\phi_\delta(\epsilon x, \delta z) + \dots \quad (97)$$

$$\psi = \psi_0(\epsilon x, \delta z) + \epsilon\psi_\epsilon(\epsilon x, \delta z) + \delta\psi_\delta(\epsilon x, \delta z) + \dots, \quad (98)$$

where the subscripts ϵ, δ , etc. refer to the successive terms in the expansion (and not to derivatives with respect to them). We can formally expand these using multiple spatial scales in both x and z directions and use the far-field boundary conditions to do the problem rigorously, but for brevity we will omit the details and present only the results.

To lowest order from the continuity equation, $\epsilon\phi$ and $\delta\psi$ are of the same order. Recall that for case II, b_{2x} and b_{2z} are both $O(\epsilon)$, whereas for case III, b_{2x} is $O(\epsilon)$ and b_{2z} is $O(1)$. Using the thermal wind equation we see that a balance to lowest order is possible in case II only if $b_{2x}\psi_x$ balances ϕ_z , or

$$\delta = \epsilon^{3/2} \quad (99)$$

so that ϕ_0 is $O(\epsilon^{1/2})$ smaller than ψ_0 . In case III, with b_{2z} of $O(1)$, the dominant balance implies $\delta = \epsilon$. In physical terms this suggests that the isopycnals are more constrained in the horizontal in case II than in

case III; that is, the domain of influence in the vertical in the stratified layer is deeper for case II. The condition that the vertical displacement ψ is assumed to be continuous at the interface leads to the results that for case II, $\check{\psi}$ is at most $O(\epsilon)$ and so $\check{\phi}$ is at most $O(\epsilon^{1.5})$, and for case III, both $\check{\psi}$ and $\check{\phi}$ are at most $O(\epsilon)$.

The above scaling effectively decouples the Margules' relation at the lowest order up to $O(\epsilon)$ for case II, and

$$C = v_{\text{jump}} + \epsilon x v'_1 - \epsilon b'_1 + O(\epsilon^2), \quad (100)$$

which leads to

$$\epsilon(C' - v'_1) = \epsilon v'_{\text{jump}} + \epsilon^2 x v''_1 - \epsilon^2 b''_1 + O(\epsilon^3). \quad (101)$$

The rhs of (101) is $O(\epsilon^2)$. With (87), this implies that $\check{\psi} = \psi$ is $O(\epsilon^2)$; hence for case II, $\check{\phi}$ is $O(\epsilon^{2.5})$. How is case III different? For case III, we can use (94) and (86) to write

$$C = v_{\text{jump}} + \epsilon x v'_1 - \epsilon b'_1 - \check{\phi}(\epsilon \hat{x}) + O(\epsilon^2), \quad (102)$$

where $\check{\phi}(\epsilon \hat{x})$ has been expanded in terms of $\epsilon \hat{x}$. Again, in case III

$$\epsilon(C' - v'_1) = \epsilon v'_{\text{jump}} + \epsilon^2 x v''_1 - \epsilon^2 b''_1 - \epsilon \check{\phi}' + O(\epsilon^3), \quad (103)$$

in which the rhs terms are all $O(\epsilon^2)$. Thus for case III, $\check{\psi} = \psi$ is $O(\epsilon^2)$; hence $\check{\phi}$ is $O(\epsilon^2)$. Thus the solution for ϕ for both cases II and III is given by

$$\phi = v_{\text{jump}}(\hat{x}) - b_{1x}(1 + z) + O(\epsilon^2). \quad (104)$$

Also, ψ occurs in the mixed layer at $O(\epsilon^2)$. To get the solution for ψ in the mixed layer to $O(\epsilon^2)$, we can either include $O(\epsilon^2)$ terms in (87) or use continuity to get

$$\psi = z(b_{1xx} - v_{\text{jump},x}) + \frac{1}{2} b_{1xx} z^2 + O(\epsilon^3). \quad (105)$$

Notice that C enters in cases II and III at $O(\epsilon)$ in contrast with case I where it occurs at $O(\epsilon^2)$. At the interface, the displacement at ϵ^2 is given by $\psi = -b''_1/2 + v'_{\text{jump}}$, where both terms on the rhs have opposing tendencies as far as the deepening and/or rising of the interface is concerned and the result depends on the assumed profile for the initial conditions. Again, we can check for continuity, for example, $\int_{-1}^0 \phi(0, z) dz = v_{\text{jump}}(0) - 1/2 b_{1x}(0) = \int_{-\infty}^0 \psi(x, z = -1)$. For case II, with profile (76) and with scaled slope s of $O(1)$, the displacement of the interface occurs at $O(\epsilon^3)$. In case III, with the profile before mixing given by (77), the interface is displaced by $\epsilon^2 \text{sech}^2 \epsilon x \tanh \epsilon x [(1 - e^{-\beta})/\beta^2 - (1 + e^{-\beta})/(2\beta)]$, which shallows on the more buoyant side and deepens on the heavier side. For small β it occurs at $O(\epsilon^2\beta)$.

The displacements in the mixed layer for cases II and III are now given by (104) and (105). These lowest-order solutions are schematically sketched in Fig. 6. The pivoting surface is given by

$$z = -1 + \frac{v_{\text{jump}}}{b_{1x}} \quad (106)$$

for both cases II and III, and

$$z_{\text{pivot}} = -\frac{1}{2} + O(\epsilon) \quad (107)$$

for case II, where (107) has been derived by recognizing that from the thermal wind relation $[0 - v_2(\hat{x})] = b_{1x}$ and $v_{\text{jump}}(\hat{x}) = -v_2(\hat{x})/2$ to the lowest order. Therefore, to this order, for case II, the isopycnals are just pivoted at middepth and undergo horizontal displacements of $O(\epsilon)$ about this pivot location. In case III, $z_{\text{pivot}} = -1 + 1/\beta - e^{-\beta}/(1 - e^{-\beta})$, which is $-1/2 - \beta/12$ for small β . In Ou (1984), the pivoting surface is at middepth to the lowest order, but with initial conditions at rest.

The restratification in cases II and III tends to restore the original tilted position of the isopycnals, but only partially. For example, in case II to restore the isopycnals the displacement needed at $z = -1$ is $1/2s$ where s , which is $O(1)$, is the scaled slope before mixing, whereas after the adjustment, the isopycnals have moved only by a distance $b_{1x}/2$.

In all cases, there is a pivoting surface in the adjusted state at which there are no horizontal displacements, but this pivot surface is not the same as the surface on which there are no horizontal pressure gradients initially (after mixing). This is due to radiation of inertial waves; the final pivot surface cannot be predicted without solving for the adjusted state.

5. Discussion and conclusions

- The mixed layer restratification is given for this wide-front problem by $b_z = -b_x \phi_z = b_x^2/f^2$, or with $M^2 = |b_x|$,

$$N^2 = \frac{M^4}{f^2}. \quad (108)$$

This simple scaling can thus be employed in GCMs with stratification-dependent parameterizations, particularly in frontal regions.

- To the lowest order, $Ri = 1$, so the restratification and Ri are the same to the lowest order as for the constant-depth problem (Tandon and Garrett 1994).

- The major assumption in this study is that of a wide front [or $\epsilon = \sqrt{\Delta b \bar{h}}/(fL)$ is small]. This is not a very restrictive condition. In FASINEX (Weller 1991), temperature variations of 1 K were seen over 20 km, and with $\alpha = 2 \times 10^{-4} \text{ K}^{-1}$, $f = 10^{-4} \text{ s}^{-1}$, and $\bar{h} = 100 \text{ m}$, we have $\epsilon = 0.2$. For the shelf-slope front shown in Fig. 10 of Ou (1984) (adapted from Marra et al. 1982), the overall variation is 0.4 kg m^{-3} over 30 km, and with $f = 9 \times 10^{-5} \text{ s}^{-1}$ this also gives $\epsilon = 0.2$. For stronger and narrower fronts, ϵ can be larger, as in Fig. 5a of Samelson and Paulson (1988), where the tem-

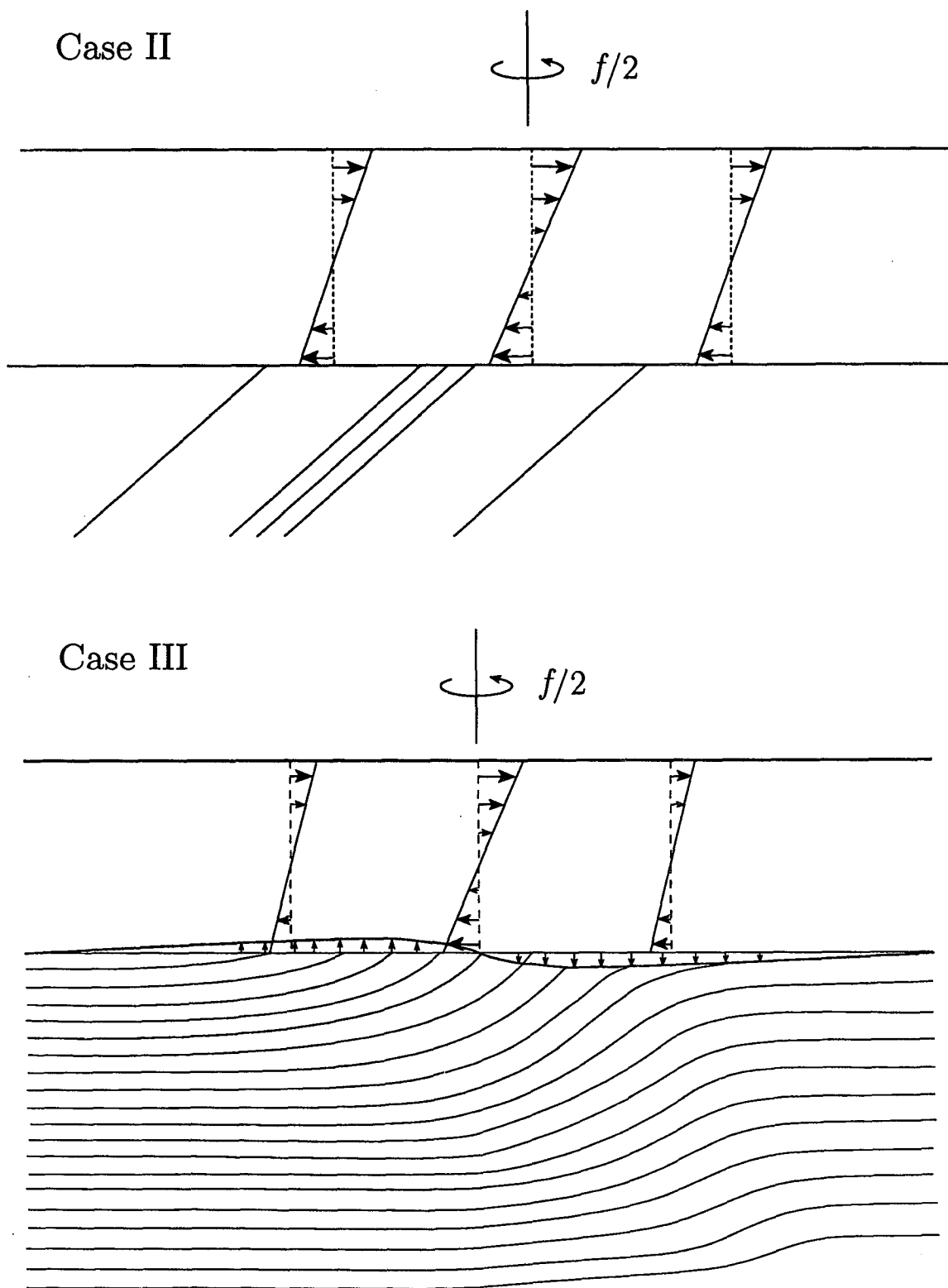


FIG. 6. Lowest-order solutions for isopycnal displacements for cases II and III.

perature changes by 1.6 K over 5.7 km, with $f = 7.3 \times 10^{-5} \text{ s}^{-1}$ (near 30°N) and $h = 30 \text{ m}$ so that, with $\alpha = 2.6 \times 10^{-4} \text{ K}^{-1}$, $\epsilon = 0.85$. Certainly, as ϵ approaches 1, the results are not strictly valid, but calculations show that the metric for restratification (108) still gives the right order of magnitude results for the last example.

- If we assume that throughout this geostrophic adjustment the Richardson number across the base of the mixed layer is maintained constant (Price et al. 1986), then we can derive an expression for thickness of the transition layer. For all cases the velocity difference across the interface is of the order $\epsilon f \lambda$. For cases I and III, b_{jump} is of the order Δb (assuming $b_z h$ is of order Δb in case III), then the transition layer thickness is $O(\epsilon^2 h)$, which is small. For case II, the velocity jump is still $\epsilon f \lambda$, but the buoyancy jump at the base of the mixed layer is $O(\epsilon \Delta b)$ [e.g., in (76)] and therefore the transition layer thickness is $O(\epsilon h)$. [Note that this result is valid for scaled slope s in case II assumed to be $O(1)$. We expect case II to become more like case III for small s , since v_{jump} will remain small and the buoyancy jump will increase, so the transition layer thickness will be smaller for small s .] In all three cases the transition layer thickness is small, so the metric for restratification and $\text{Ri} = 1$ probably carry over to realistic conditions.

- Young (1994) considers a mixed layer model formulation that incorporates dynamics due to horizontal buoyancy gradients. In his model, the vertical homogeneity is restored by intermittent mixing events, and the momentum and density relax to their averaged values in between these events. In this paper, the horizontal gradients in the mixed layer result in dynamics at an order lower than the quasigeostrophic approach. The resulting subinertial dynamics and its instabilities are considered in Young (1994) and Young and Chen (1994).

If the relaxation times of momentum and density are taken to be the same, then the restratification achieved in this paper and in Young (1994) are the same. However, Young's formulation assumes that the difference in the mixed layer depth across the front is small and that the mixed layer overlies a much denser homogeneous layer such that the buoyancy difference in the horizontal is much smaller than the buoyancy jump in the vertical, at the base of the mixed layer. With a *finite* change in the mixed layer depth and with the buoyancy difference in the horizontal the *same* as that at the mixed layer base, the results are similar (our formulation is for the inviscid restratification after a single event). Thus, it may be possible to reconsider the dynamics in the mixed layer for an ensemble of events as in Young (1994) but with finite variations in the mixed layer depth and a buoyancy jump at the base of the mixed layer of the same order as the buoyancy difference in the horizontal, with the mixed layer overlying a *stratified* layer.

- We have shown that Ri is $O(1)$ in the mixed layer. It would be interesting to examine whether this system is baroclinically unstable. Stone (1970) shows that for $0.25 < \text{Ri} < 0.95$, symmetric instabilities are most unstable and for $\text{Ri} > 0.95$ conventional Eady instability (which exists for $\text{Ri} > 0.86$, e.g., Pedlosky 1987) dominates. Thus we expect that the region of maximum horizontal gradients may be particularly susceptible to the nongeostrophic symmetric instability. The effect of nonuniform velocity shear (and presence of an inflection point in it) may enhance these instabilities. In a previous treatment of instabilities of a mixed layer front via a continuously stratified model (Samelson 1993) symmetric instabilities have not been considered. We plan to consider these, but the analysis is beyond the scope of the present paper.

Acknowledgments. The authors are grateful to William R. Young for providing preprints of his papers and for interesting discussions on this subject. This work is supported by the UCAR fellowship program in ocean modeling and additionally by ONR and by NSERC and DFO of Canada.

APPENDIX

Case I with Arbitrary $b(x)$ in the Mixed Layer

Consider the mixed layer in case I to have an arbitrary buoyancy initial distribution that slowly varies across the front; that is, $b = b(\epsilon x)$ [unrelated to $h(x)$] in the mixed layer, and $b = N^2 z$ below.

Following the nondimensionalization and the procedure for case I results in

$$C(\epsilon \hat{x}) = -[b_x h + h_x(h + b_x)]. \quad (109)$$

The solution for displacements in the mixed layer is then

$$\phi = -b_x(z + h) - hh_x - bh_x, \quad (110)$$

$$\psi = z[b_{xx}h + b_x h_x + h_{xx}(b + h) + h_x(b_x + h_x)] + \frac{1}{4} b_{xx} z^2. \quad (111)$$

For instance, if we consider a modification of the problem in Ou (1984), where instead of a rigid bottom we consider the mixed layer overlying a stratified layer, then $h_x = 0$, $\phi = -b_x(z + h)$ and the isopycnals are pivoted at the interface. The top surface has no vertical displacements, but has maximum horizontal displacements. In the final state, $\psi = z b_{xx} h + 1/4 b_{xx} z^2$ and therefore, the interface deepens on the denser side and rises on the lighter side.

REFERENCES

- Gill, A. E., 1981: Homogeneous intrusions in a rotating stratified fluid. *J. Fluid Mech.*, **103**, 275–295.
 —, 1982: *Atmosphere-Ocean Dynamics*. Academic Press, 662 pp.

- Marra, J., R. W. Houghton, D. C. Boardman, and P. J. Neale, 1982: Variability in surface chlorophyll *a* at a shelf-break front. *J. Mar. Res.*, **40**, 575–591.
- Olbers, D. J., 1983: Models of the oceanic internal wave field. *Rev. Geophys. Space Phys.*, **21**, 1567–1606.
- Ou, H. W., 1984: Geostrophic adjustment: A mechanism for frontogenesis. *J. Phys. Oceanogr.*, **14**, 994–1000.
- , 1986: On the energy conversion during geostrophic adjustment. *J. Phys. Oceanogr.*, **16**, 2203–2204.
- Pedlosky, J., 1987: *Geophysical Fluid Dynamics*, Springer-Verlag, 710 pp.
- Price, J. F., R. A. Weller, and R. Pinkel, 1986: Diurnal cycling: Observations and models of the upper ocean response to diurnal heating, cooling, and wind mixing. *J. Geophys. Res.*, **91**, 8411–8427.
- Ripa, P., 1993: Conservation laws for primitive equations models with inhomogeneous layers. *Geophys. Astrophys. Fluid Dyn.*, **70**, 85–111.
- Samelson, R. M., 1993: Linear instability of a mixed-layer front. *J. Geophys. Res.*, **98**, 10 195–10 204.
- , and C. P. Paulson, 1988: Towed thermistor chain observations of fronts in the subtropical North Pacific. *J. Geophys. Res.*, **93**, 2237–2246.
- Stone, P. H., 1970: On non-geostrophic baroclinic instability: Part II. *J. Atmos. Sci.*, **27**, 721–726.
- Tandon, A., and C. Garrett, 1994: Mixed layer restratification due to a horizontal density gradient. *J. Phys. Oceanogr.*, **24**, 1419–1424.
- Weller, R. A., 1991: Overview of the frontal air–sea interaction experiment (FASINEX): A study of air–sea interaction in a region of strong oceanic gradients. *J. Geophys. Res.*, **96**, 8501–8516.
- Young, W. R., 1994: The subinertial mixed layer approximation. *J. Phys. Oceanogr.*, **24**, 1812–1826.
- , and L. Chen, 1994: Baroclinic instability and thermohaline gradient alignment in the mixed layer. *J. Phys. Oceanogr.*, in press.